Journal of Electrical and Electronics Engineering Research

Volume 6 Number 2 August 2014
ISSN 1993-8225

Academic Journals

ABOUT JEEER

The Journal of Electrical and Electronics Engineering Research is published monthly (one volume per year) by Academic Journals.

Journal of Electrical and Electronics Engineering Research (JEEER) is an open access journal that provides rapid publication (monthly) of articles in all areas of the subject such as waste management, ozone depletion, Kinetic Processes in Materials, strength of building materials, global warming etc. The Journal welcomes the submission of manuscripts that meet the general criteria of significance and scientific excellence. Papers will be published shortly after acceptance. All articles published in JEEER are peer-reviewed.

Contact Us

Editorial Office: jeeer@academicjournals.org

Help Desk: helpdesk@academicjournals.org

Website: http://www.academicjournals.org/journal/JEEER

Submit manuscript online http://ms.academicjournals.me/

Editors

Editorial Board

Journal of Electrical and Electronics Engineering Research

Table of Contents: Volume 6 Number 2 August 2014

ARTICLES

Research Articles

academicJournals

Vol. 6(2), pp. 6-12, August, 2014
DOI 10.5897/JEEER2014.0504
Article Number:EAB4EFC46665
ISSN 1993–8225

http://www.academicjournals.org/JEEER

Journal of Electrical and Electronics Engineering Research

Full Length Research Paper

Reduction of side lobe level in non-uniform circular antenna arrays using the simulated annealing algorithm

A. Zangene[1]*, H. R. Dalili Oskouei[2] and M. Nourhoseini[3]

[1]Amirkabir University of Technology, Tehran, Iran.
[2]University of Aeronautical Science and Technology (Shahid Sattari), Tehran, Iran
[3]Amirkabir University of Technology, Tehran, Iran.

Received 8 April, 2014; Accepted 29 July, 2014.

This paper investigates the reduction of side lobe level in antenna arrays. Reduction of side lobe level in antenna arrays has some limitations including fixed width of the beam. We have modeled the side lobe level reduction as an optimization problem using simulated annealing technique for side lobe level reduction of a specific beam width. The advantage of this method compared with other methods is that it can get out of local minimums and converge to the optimized answer. Efficiency of simulated annealing algorithm in pattern extraction of desired circular antenna, which is used frequently in modern telecommunication and radar systems, is investigated and the results are compared with that of genetic and evolutionary algorithms.

Key words: Simulated annealing, antenna array, circular array, non-uniform antenna array, side lobe level.

INTRODUCTION

Antenna arrays have various applications in wireless and mobile communication systems. In most application antenna should be designed in such a way that it can transmit produced beam in various directions and distances. To fulfill this goal, an array of antennas must be used. Higher transmission power, lower power consumption, radiating beam control, and higher efficiency can be obtained using antenna arrays. Arrays can have different forms such as linear, circular, and planar with different applications, like radar, sonar, imaging, biomedicine and mobile communications (Panduro et al., 2006; Balanis, 1997; Shihab et al., 2008 and Dessouky et al., 2006).

Due to the particular structure of circular antenna, attention toward circular arrays has increased in recent studies, (Panduro et al., 2006); Shihab et al., 2008; Dessouky et al., 2006; Pathak et al., 2009). In circular antenna arrays with non-uniform distribution, elements are placed on a circular ring with non-uniform distances (Figure 1).

This group of antennas has important functionality with different applications such as radio navigation, air and space navigation, sound tracking, etc (Dessouky et al., 2006; Granville et al., 1994; Locatelli et al., 1994; Ingber, 1993; Aydin and Fogarty, 2004). Recently, antenna arrays have been suggested for wireless communications especially as intelligent antennas. In many studies (Panduro et al., 2006; Balanis, 1997; Shihab et al., 2008;

*Corresponding author. E-mail: Amirhosein@aut.ac.ir

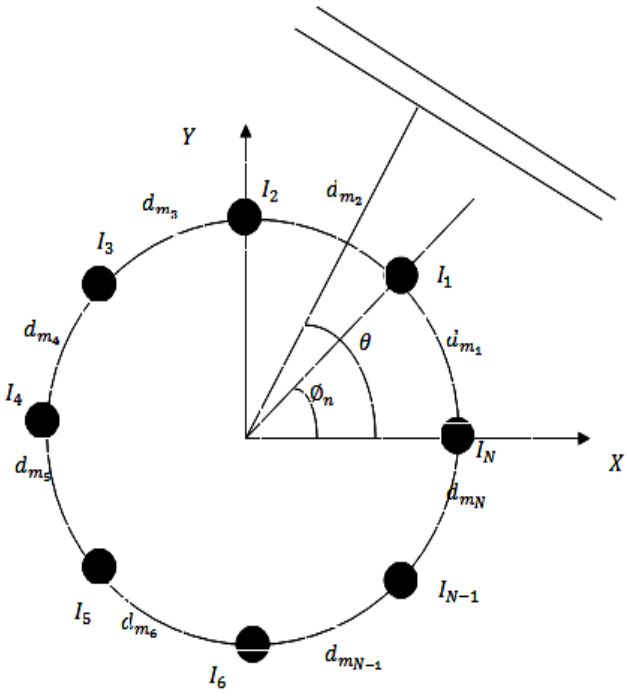

Figure 1. Structure of an antenna array with n elements (Panduro et al., 2006).

Dessouky et al., 2006; Pathak et al., 2009) it has been tried to reduce side lobe level as much as possible in non-uniform distribution state. Reduction of side lobe level has ideal influences on telecommunication systems.

Genetic and evolutionary algorithms have been used to reduce side lobe level in paper (Panduro et al., 2006; Shihab et al., 2008). Various parameters such as beam width, and noise sensitivity, and some other factors (antenna gain, radiation pattern, antenna size) should be considered to reduce side lobe level. The objective of this problem is to find the best distances between elements and the stimulation amplitude of each element so that side lobe level is minimal.

Therefore, the problem of finding the best set of distances between elements and their stimulation amplitude can be proposed as an optimization problem. Here, we have used simulated annealing technique to specify the best distances between elements and their stimulation amplitude so that the final produced pattern will have the maximum reduction in side lobe level. Simulated annealing algorithm adds a random aspect to the descent along with the gradient which is controllable by the T (temperature) parameter. This algorithm allows both transitions to the higher energy state or to the lower energy state; therefore using this algorithm, it is possible to get out of local minimums and get to the global optimized answer. In our experiments beam width and the main beam formation angle were fixed to 50 and 0° respectively.

PROBLEM STATEMENT

Suppose that n isotropic elements with interspaces d_m are placed on the circumference of a circular ring with radius *a* on x-y plane (Figure 1). Assuming that elements are isotropic, it can be concluded that the propagation pattern of this array of antennas can be explained by its array factor.

Array factor for a circular array on x-y plane is stated as below (2):

$$AF(\theta, I, d_m) = \sum_{n=1}^{N} I_n e^{jka(\cos(\theta-\theta_0)-\cos(\theta_0-\phi_n))} \quad (1)$$

In which:

$$ka = \frac{2\pi a}{\lambda} = \sum_{i=1}^{N} d_{m_i} \quad (2)$$

$$\phi_n = \frac{(2\pi \sum_{i=1}^{n} d_{m_i})}{\sum_{i=1}^{N} d_{m_i}} \quad (3)$$

θ is the angle at which the main beam is generated, d_m (a 1*10 matrix) is the distance between antenna array elements, and I_m, which is also a 1*10 matrix, is the stimulation amplitude of each element.

In the d_m array, each component d_{m_i} is the distance of the ith element from the (i+1)th one.

$k = \frac{2\pi a}{\lambda}$ is the constant value of the phase difference between elements, θ is the intersection angle of the beam with x-y plane, λ is the beam wave length, and θ_0 is the angle at which the main beam has the most propagation. As indicated before, finding the best set of places and stimulation amplitude of the elements can be proposed as an optimization problem. Therefore, to solve this problem using the simulated annealing algorithm, an objective function must be defined through which the simulated annealing algorithm can get to the optimized answer. Assuming that θ_0 is the angle at which the maximum propagation occurs and θ varies in the range [-π,π], θ_{msl} is the angle at which the first side lobe, which is the highest one, is generated, $BWFN_{desired}$ is the width of the desired beam, which assumed to be equal to the constant value 50, and BWFN (I, d_m) is the first null beam width, the objective function is stated as follows:

$$f_1 = \frac{\left|AF(\theta_{msl1}, I, d_m) + AF(\theta_{msl2}, I, d_m) + AF(\theta_{msl3}, I, d_m)\right|}{AF(\theta_0, I, d_m)} + \left|BWFN_{desired} - BWFN(I, d_m)\right| \quad (4)$$

Based on the defined objective function, the best set of I and d_m is obtained when f_1 is minimal. Reduction of all side lobes is considered at the same time using the defined objective function.

In this problem, it is also assumed that the circumference of the circle on which the elements are located is constant.

THE PROPOSED ALGORITHM

The main objective of this work is to maximally reduce side lobes for a circular antenna array in which elements are distributed non-normally. There are some limitations to maximally reduce side lobes in a circular antenna array such as constant width of the desired beam, number of elements and the circumference.

Simulated annealing which is used in this paper is a generic probabilistic met heuristic method for obtaining optimized main point for the desired objective function in a large search space which was first presented by Kirkpatrick in 1983 (Pathak et al., 2009). This method is usually used when the search space is discrete. For some specific problems, simulated annealing technique can be more efficient than searching the whole state space. It may be possible to obtain the best answer by searching the whole space state, but it is not possible considering the time needed for the process. Furthermore, most of the time, we get the answer which is close to the best answer in a specific period of time.

The name and idea of this algorithm has been extracted from the annealing technique in metallurgy. In this process, metal is heated to the melting temperature and then is cooled gradually under control. Heating causes the atoms in the crystalline structure of the metal to leave their primary position (primary positions are considered as local minimums) and place randomly in new locations. Then, in the gradual cooling process, the states with lower energy levels with respect to the primary state of the metal have more chances of converging.

In this technique, any point in the search space is considered as a state with energy E. when the system transits from one state to another, the probability of accepting the new state is defined by P ($E_{current}$, E_{new}, T) which depends on the current state energy, new state energy, and the parameter T. In this algorithm, if the new state energy is lower than the current state energy, current state to new state transition is done with the probability of 1.

$$\Delta E = E_{new} - E_{current} \quad (5)$$

$$\rho(\Delta E) = \begin{cases} e^{\frac{-\Delta E}{T}} & \Delta E > 0 \\ 1 & \Delta E <= 0 \end{cases} \quad (6)$$

And if the new state energy is equal to or higher than the current state energy, algorithm accepts this state transition with the probability of $e^{\frac{-\Delta E}{T}}$ which is dependent on parameter T. At first, this probability has the maximum value and gradually after running the algorithm when $T \to 0$, it tends toward zero. Transition to higher energy states, provides the possibility of getting out of local minimums for the algorithm (Smith et al., 1998; Koulmas et al., 1994; Kirkpatrick et al., 1983).

It can be shown that for any finite problem, the probability that the simulated annealing algorithm will give an answer close to the total optimized answer, with the assumption of no time limitation, tends to zero (Granville et al., 1994; Locatelli, 2001).

It is also possible to use an adaptive neighborhood in this algorithm; so that the neighborhood radius will accept all the states at the beginning and continuing the algorithm it is reduced gradually until converging to the best answer in the end. Simulated annealing algorithm with adaptive neighborhood radius is applicable when the distance between the optimized answer and the current answer is shorter than the step length (Ingber, 1993). The Flow chart of our proposed algorithm for solving side lobe reduction problem is shown in Figure 2.

Based on this technique, it is possible to search the whole state space normally in the primary stages and to reduce the search space to obtain the best answer during the algorithm process. In reference (Aydin and Fogarty, 2004), a number of advantages and disadvantages of the simulated annealing technique have been proposed. This technique has been used for solving major and practical problems such as flow shop scheduling (Low, 2005; Burke et al., 2003), time tabling (Framinana and Schusterb, 2006; Cerny, 1985), travelling salesman (Lin and Kernighan, 1973; Salcedo-Sanz et al., 2004), communication systems (Paik and Soni, 2007; Locatelli, 2000), continuous optimization, and etc.

RESULTS AND DISCUSSION

The presented algorithm in the previous part was implemented and the results were studied for the design of a circular antenna array with non-normal distribution. In the experiments, to maximally reduce side lobes, the angle with maximum propagation was assumed to be zero at $\theta_0 = 0$. The experiments were carried out for different number of elements 8, 10, and 12 and the resulted array factor for each one was reported.

Variation distance value and the coefficient, which was used for gradual cooling in the algorithm, was set to 0.01

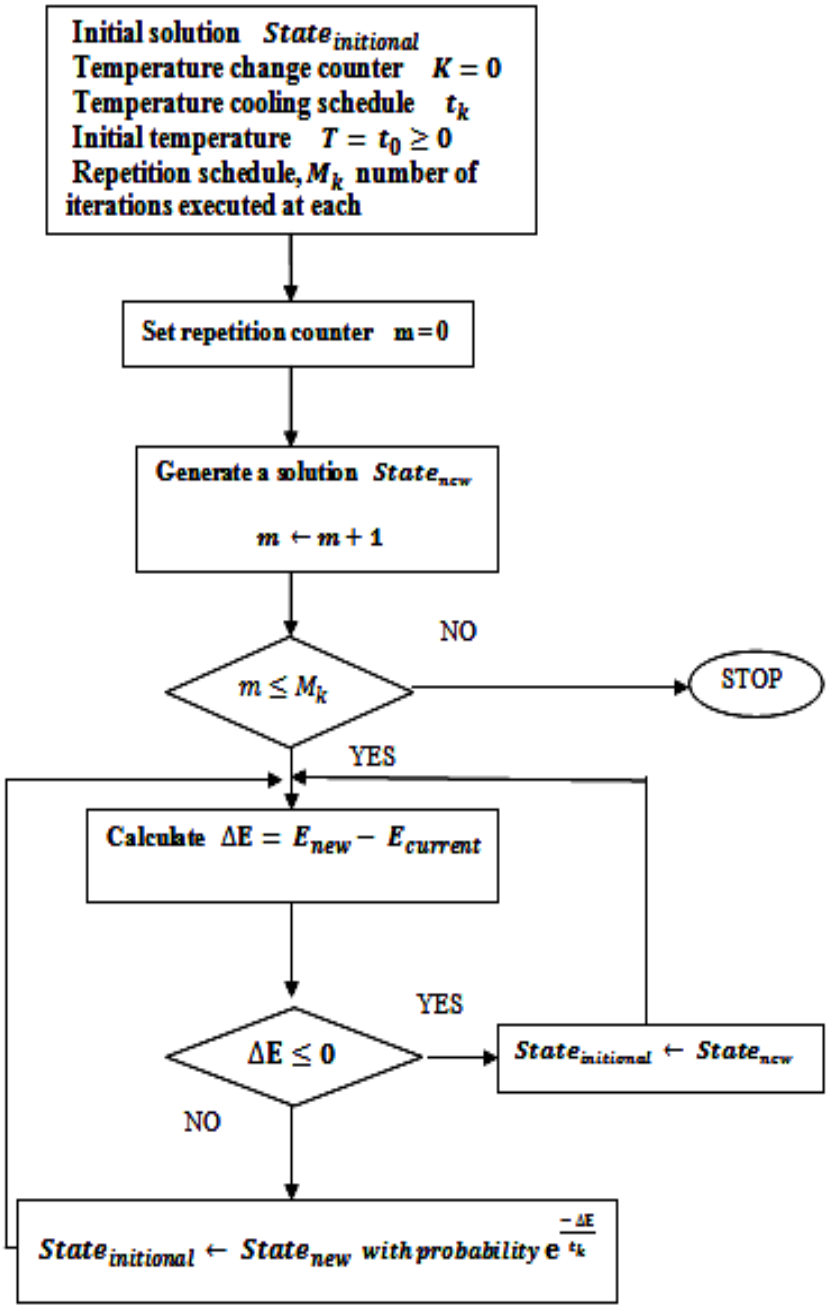

Figure 1. Flow chart for the simulated annealing algorithm.

and 0.7 respectively in the implementation of the simulated annealing algorithm. The algorithm continues until 5 successive output values converge to a unit value. Maximum number of repetitions is assumed to be 10000. As seen in the Figures 3 and 4, for 10 elements, the first side lobe level by using the normal distribution, the genetic algorithm and the proposed algorithm is -7.9, -11.1 and -11.9 dB respectively. In conclusion, by using the simulated annealing algorithm, the side lobe level with respect to the main lobe has 0.8dB reduction in comparison to the genetic algorithm and 4.1 d B reduction in comparison to the algorithm of normal distribution of elements.

According to the results, superiority of this algorithm in comparison to the genetic algorithm can be observed, because the Genetic algorithm may fall in local minimums while the simulated annealing algorithm can converge to an optimized answer by starting from an appropriate primary point and by some repetitions. In Figures 5 and 6, propagation patterns for an antenna array with 12

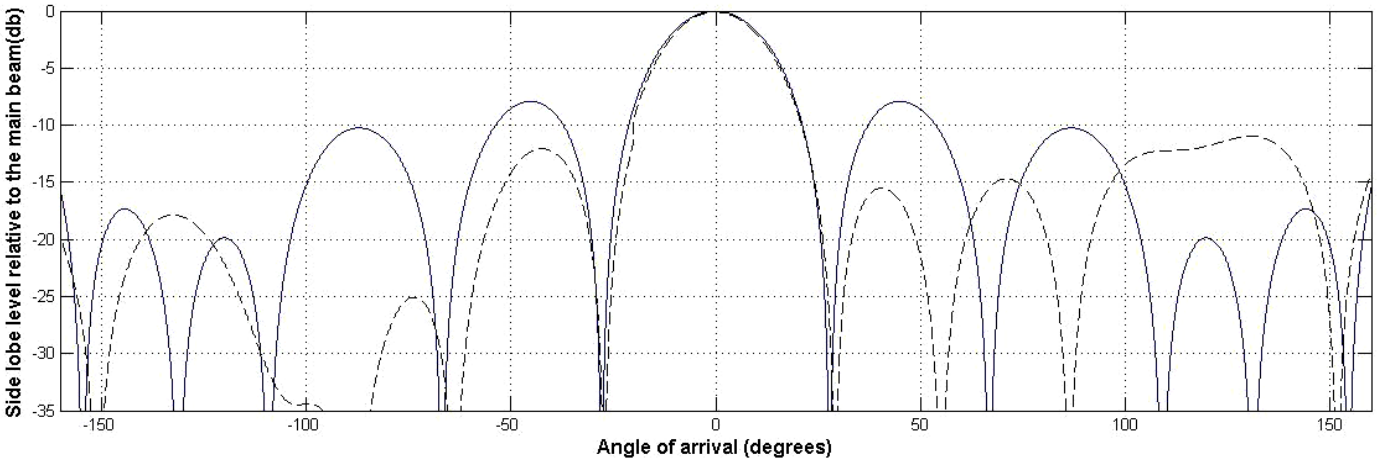

Figure 3. Comparison between propagation patterns of normal distribution (——) of elements and simulated annealing algorithms (-----) for an antenna array with 10 elements.

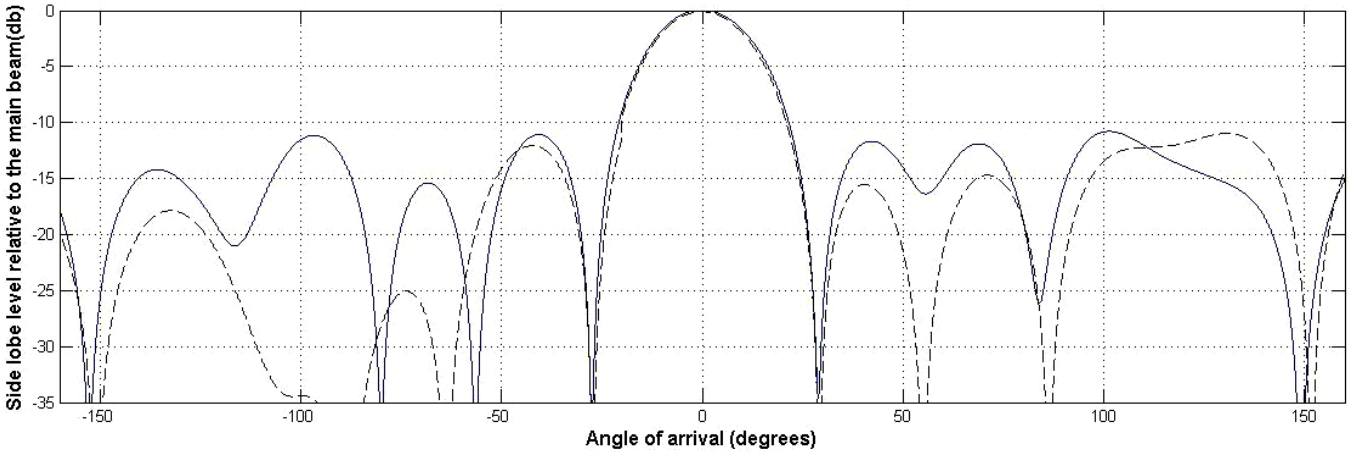

Figure 4. Comparison between propagation patterns of genetic (——) and simulated annealing algorithms (- - - - -) for an antenna array with 10 elements.

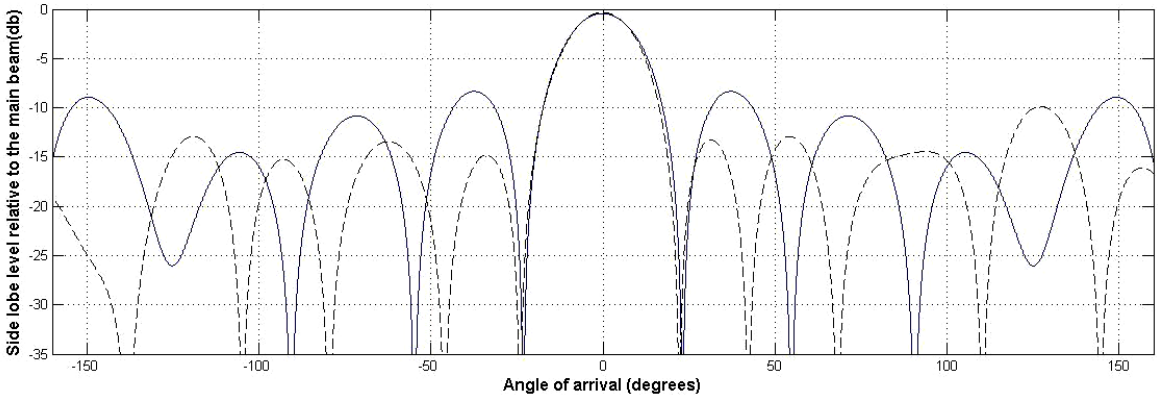

Figure 5. Comparison between propagation patterns of normal distribution of elements (——) and simulated annealing algorithms (- - - - -) for an antenna array with 12 elements.

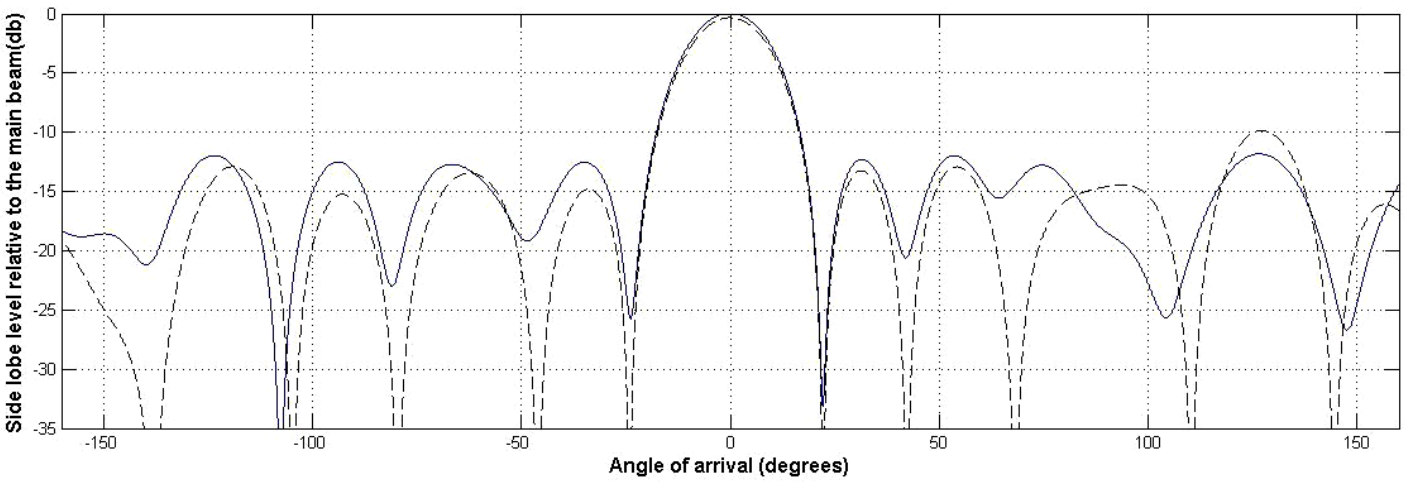

Figure 6. Comparison between propagation patterns of Genetic (——) and simulated annealing algorithms (- - - - -) for an antenna array with 12 element

Table 1. Examples for the non-normal distribution of antenna array elements on a circular surface for two different numbers of elements.

N	SLL(dB)	BWFN(deg)	$d_{m_1}, d_{m_2}, d_{m_3}, \ldots, d_{m_N}; I_1, I_2, I_3, \ldots, I_N$	Aperture
8	-10.5	71.5	0.05961 λ , 0.314 λ , 0.7763 λ , 0.7425 λ , 0.6297 λ , 0.8969 λ , 0.4633 λ , 0.5267 λ , 0.3289 , 0.2537 , 0.7849 , 1 , 1.0171 , 0.5183 , 0.5176 , 0.4612	4.40 λ
10	-11.9	55.3	0.3258 λ , 0.4934 λ , 0.3505 λ ,1.6573 λ , 0.6213 λ , 0.9948 λ , 0.4968 λ , 0.2431 λ , 0.5878 λ , 0.3148 λ , 0.9845 , 0.3883 , 0.4092 , 0.9674 , 0.6586 , 0.5533 , 0.5834 , 0.6215 , 0.4665 , 0.6148	6.08 λ
12	-15	45.6	0.5181 λ , 0.3665 λ , 1.4283 λ , 0.8367 λ , 0.3249 λ ,0.5702 λ , 0.4983 λ , 0.8135 λ , 0.8195 λ , 0.4992 λ , 0.3595 λ , 0.7370 λ , 0.1864 , 0.5116 , 0.2046 , 0.6486 , 0.7512 , 0.8393 , 0.5577 , 0.4095 , 0.5225 , 0.4875 , 0.4833 , 0.8453	7.07 λ

elements are shown. In these figures, the propagation pattern obtained from the simulated annealing algorithm is compared with the patterns obtained from normal distribution of elements and the genetic algorithm in Figure 5 and 6 respectably.

As seen in the figures, the first side lobe level is -15 dB for the simulated annealing algorithm,-12.8 dB for the genetic, and -7 dB for normal distribution of elements. Therefore we have 1.2 and 5 dB reduction in first side lobe using simulated annealing algorithm in comparison of genetic algorithm and normal distribution of 12 elements (Panduro et al., 2006).

Results obtained from simulated annealing algorithm for distribution of elements on a circular array with their distance $\{d_{m_i}\}$, amplitude $\{I_i\}$ for a set of 8, 10 and 12 elements are presented. In Table 1, Based on the results, by increasing the number of elements and the circumference of the circle on which elements are placed, side lobe levels reduce.

Conclusion

In this paper, simulated annealing algorithm has been used for maximally reducing side lobes in circular antenna arrays with non-normal distribution of elements with the assumption of constant beam width. Simulated annealing algorithm can converge to an optimized answer by starting from an appropriate primary point and by some repetitions. This algorithm can provide the possibility of getting out of local minimums and converging to the local optimized answer by adding a probability aspect to the descent along with the gradient.

Based on the obtained results from the experiments, the efficiency of this algorithm in getting out of local minimums (the genetic algorithm may get stuck in local minimums) and getting to a close optimized answer has been demonstrated.

In conclusion, simulated annealing algorithm shows better efficiency and reduction in side lobes in comparison to the other methods.

Conflict of Interest

The authors have not declared any conflict of interest.

ACKNOWLEDGEMENT

This research is supported by the Iran Telecommunication Research Center and the authors gratefully acknowledge the institute.

REFERENCES

Panduro M, Mendez A, Dominguez R, Romero G (2006). Design of non-uniform circular antenna arrays for side lobe reduction using the method of genetic algorithms, Int. J. Electron. Commun. (AEU) 60:713-717. http://dx.doi.org/10.1016/j.aeue.2006.03.006

Balanis CA (1997). Antenna Theory: Analysis and Design, John Wiley & Sons, New York.

Shihab M, Najjar Y, Dib N, Khodier M (2008). Design of non -uniform circular antenna arrays using particle swarm optimization, J. Elect. Eng. 59(4):216-220.

Dessouky M, Sharshar H, Albagory Y (2006). Efficient Side lobe Reduction Technique For Small-Sized Concentric Circular Arrays, Progress In Electromagnetics Res. PIER 65:187-200. http://dx.doi.org/10.2528/PIER06092503

Granville V, Krivanek M, Rasson JP (1994). Simulated annealing, A proof of convergence, IEEE Transactions On Pattern Analysis and Machine Intelligence, 16:652. http://dx.doi.org/10.1109/34.295910

Locatelli M (2001).Convergence and first hitting time of simulated annealing algorithms for continuous global optimization. Math. Methods. Oper. Res. 54:171-199. http://dx.doi.org/10.1007/s001860100149

Ingber L (1993). Simulated annealing: practice versus theory, J. Math. Comput. Model.18(11):29-57. http://dx.doi.org/10.1016/0895-7177(93)90204-C

Aydin ME, Fogarty TC (2004). A distributed evolutionary simulated annealingalgorithm for combinatorial optimisation problems, J. Heuristics 10:269-292. http://dx.doi.org/10.1023/B:HEUR.0000026896.44360.f9

Low CY (2005). Simulated annealing heuristic forflowshop scheduling problems withunrelated parallel machines, Comput. Operat. Res. 32:2013-2025. http://dx.doi.org/10.1016/j.cor.2004.01.003

Burke EK, Eckersley A, McCollum B (2003). Using simulated annealing to studybehaviour of various exam timetabling data sets, in: Proceedings of the Fifth Meta heuristics Int. Conference (MIC 2003), Kyoto, Japan, August.

Framinana JM, Schusterb C (2006). An enhanced timetabling procedure for the nowait job shop problem: a complete local search approach, Comput. OperationsRes. 331:1200–1213.

Cerny V (1985). A thermodynamical approach to the travelling salesman problem: anefficient simulation algorithm, J. Optimization Theory Appl. 45:41-51. http://dx.doi.org/10.1007/BF00940812

Lin S, Kernighan BW (1973). An effective heuristic algorithm for the traveling salesman problem, Operations Res. 21(2):498-516. http://dx.doi.org/10.1287/opre.21.2.498

Salcedo-Sanz S, Santiago-Mozos R, Bousono-Calzon C (2004). A hybrid hopfieldnetwork-simulated annealing approach for frequency assignment in satellitecommunications systems, IEEE Trans. Syst. Man Cybernet. Part B: Cybernet. 34(2):1108-1116. http://dx.doi.org/10.1109/TSMCB.2003.821458 PMid:15376856

Paik CH, Soni S (2007). A simulated annealing based solution approach for the two layered location registration and paging areas partitioning problem in cellularmobile networks, Eur. J. Operat. Res. 178:579-594. http://dx.doi.org/10.1016/j.ejor.2006.01.039

Locatelli M (2000). Convergence of a simulated annealing algorithm for continuousglobal optimization, J. Global Optimization 18:219–234. http://dx.doi.org/10.1023/A:1008339019740

Smith K, Palaniswami M, Krishnamoorthy M (1998). "Neural techniques for combinatorial optimization with applications," Neural Networks, IEEE Transactions on, 9:1301-1318. http://dx.doi.org/10.1109/72.728380 PMid:18255811

Koulmas AC, Antony SR, Jaen R (1994). A survey of simulated annealing applications to operations research problems, Omega, 22:41. http://dx.doi.org/10.1016/0305-0483(94)90006-X

Kirkpatrick S, Gelatt CD, Vecchi MP (1983). Optimization by simulated annealing, Science 220(4598):671-680. http://dx.doi.org/10.1126/science.220.4598.671 PMid:17813860

Pathak NN, Mahanti GK, Singh SK, Mishra JK, Chakraborty A (2009). "Synthesis of thinned planar circular array antennas using modified particle swarm optimization," Progress In Electromagnetics Res. Lett. 12:87-97. http://dx.doi.org/10.2528/PIERL09090606

academicJournals

Vol. 6(2), pp. 13-20, August, 2014
DOI 10.5897/JEEER2014.0507
Article Number: BE18BD146667
ISSN 1993–8225

http://www.academicjournals.org/JEEER

Journal of Electrical and Electronics Engineering Research

Full Length Research Paper

Transformerless impedance matching networks for automotive power line communication

Peter Nisbet, Minco He and Lian Zhao*

Department of Electrical and Computer Engineering Ryerson University, ON, M5B 2K3, Canada.

Received 6 May, 2014; Accepted 29 July, 2014

The automotive industry is constantly looking for ways of improving vehicles fuel economy, reliability, and reducing cost of manufacturing and maintenance. As a result, vehicle manufacturers have looked into power line communication (PLC) technology as a possible solution. However the nature of a vehicles power lines such as extremely low impedances, time varying channel characteristics, and noise make it difficult for modems to provide reliable communication. Extensive research is being conducted to improve communication reliability over power line networks. One of the areas being studied is impedance matching. This paper examines previous impedance matching methods proposed for PLC and proposes a transformerless matching network. The transformerless topology allows for reduction in modem PCB size and for possible integration in a modem IC. Simulations are conducted on the proposed matching network to determine its ability to provide matches to impedances found on the vehicle power line. The noise characteristics of the matching network are also examined to determine the impact the circuit will have on the modem.

Key words: Transformerless, power line communication (PLC), impedance, modem.

INTRODUCTION

Power line communication (PLC) has attracted lots of attention in the automotive industry, due to the prospects of reduced weight, improved fuel efficiency, and ease of integration and maintenance (Benzi et al., 2008). Existing vehicle communication networks such as Controller Area Network (CAN) and Local Interconnect Network (LIN) require four wires to provide communication and power the modems. PLC utilizes the vehicles power lines for communication, eliminating the requirement for any extra wires except the power cable for communication.

In order to achieve the benefits of PLC in vehicles, modem designers must contend with time-varying and location-varying impedances, impulsive noise sources, and significant attenuation due to transmission distance and low impedance loads (Sun and Amaratunga, 2011). Typically modem designers have focused their efforts on developing robust modulation schemes such as orthogonal frequency division multiplexing (OFDM), frequency hop spread spectrum (FHSS) and quadrature phase shift keying (QPSK) (Maniati and Skipitaris, 2007; Fallows et al., 1998), along with improving the line drive ability of the transmitters. However, the varying nature of the power line channel impedance makes standard impedance matching networks ineffective. The lack of efficient impedance matching results in poor signal power transferred through the channel. This leads to

. *Corresponding author. Email: l5zhao@ryerson.ca

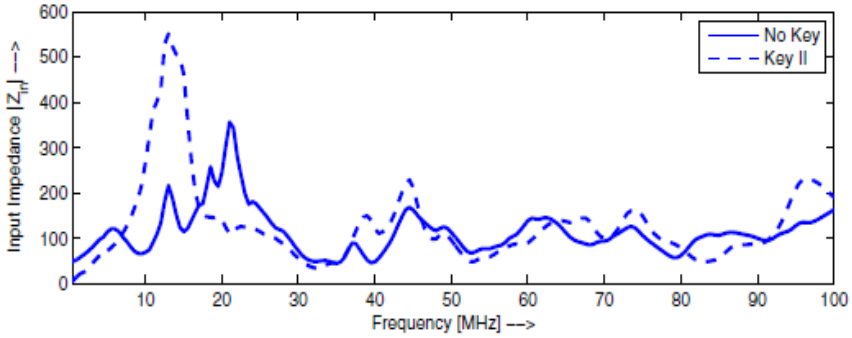

Figure 1. Impedance characteristics from 2006 Pontiac Solsctice. Input impedance for front right with ignition on and off (Mohammadi et al., 2009).

higher power consumption, reduced transmission distance, and produces reflections resulting in poor communication performance of the PLC modem (Sun and Amaratunga, 2011; Araneo et al., 2009).

There has been research to develop PLC impedance matching solutions. However most efforts are focused on AC power line networks (Antoniou, 1967; Li et al., 2004; Despande et al., 2013; Sun and Amaratunga, 2011; Choi et al., 2008; Sibanda et al., 2011). This paper will focus on automotive power line networks and propose a transformerless impedance matching solution for this application. The proposed matching networking is based on current matching network topologies and will focus on cost and IC integration and performance.

In the remaining part of this paper, background of DC power line impedance characteristics and a review of available PLC impedance matching approaches was provided. Next is a presentation of the proposed impedance matching network. This is followed by simulation results of the impedance matching network. Thereafter, the results are summarized and the paper concluded.

REVIEW OF AUTOMOTIVE POWER LINE IMPEDANCE CHARACTERISTICS

While there are similarities between AC power line impedance characteristics and automotive power line impedance characteristics, there are key differences which prevent AC power line impedance characteristics from being used directly into DC power line. The primary difference is that most devices connected to the vehicle power line have bypass capacitors. This means the power line impedance may not be purely inductive as it would be in AC power line networks. Secondly, the loads inside a car are always connected and generally will not be removed under normal operation, as opposed to AC networks where devices can be removed from the network. Thirdly, the impedance of the automotive power line changes as motors, actuators and electronic devices are turned on and off inside the car (Mohammadi et al., 2009), leading to varying channel impedance. Due to these issues, standard fixed impedance matching networks do not function well. Therefore an adaptive impedance matching network must be designed.

Vehicle power line impedance characteristics

Like AC PLC networks, the impedance characteristics of DC PLC networks are time and location varying, resulting in poor signal power being transferred to the channel (Mohammadi et al., 2009). The cause of the impedance variations is due to the activation and deactivations of motors, actuators and electronics within the vehicle during the course of operation. The state changes generate impulsive noise and change the impedance of the line. Research has been conducted to analyze the impedance characteristics of vehicle power line systems during varying states of operation.

Figure 1 shows the impedance vs. carrier frequency using a 2006 Pontiac Solsctice (Mohammadi et al., 2009) with ignition on and off. The measurements were taken from three points: front, cabin and rear of the vehicle. As can be seen from Figure 1, the impedance values change with respect to vehicle operating state along with different carrier frequencies. The magnitude of the channel impedance ranges from 10 to 600 Ω (Mohammadi et al.,2009). It is difficult to determine the complex impedance characteristics of the power line with only the magnitude shown in Figure 1. Nevertheless, from previous investigations on AC and high voltage automotive PLC, it can be assumed that the imaginary part is inductive (Choi et al., 2008).

Previous PLC impedance matching topologies

Currently, there are three popular methods for impedance matching and improving power transferring of a PLC transceiver. Several of these designs are

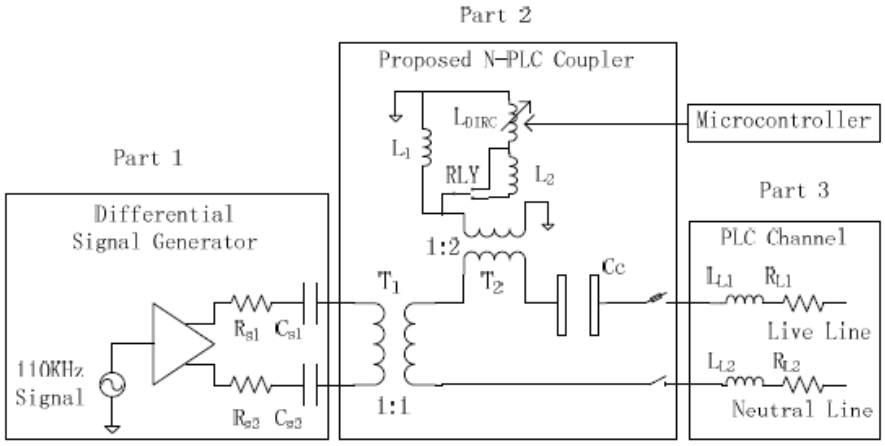

Figure 2. Adaptive impedance matching network designed in Sun and Amaratunga (2011).

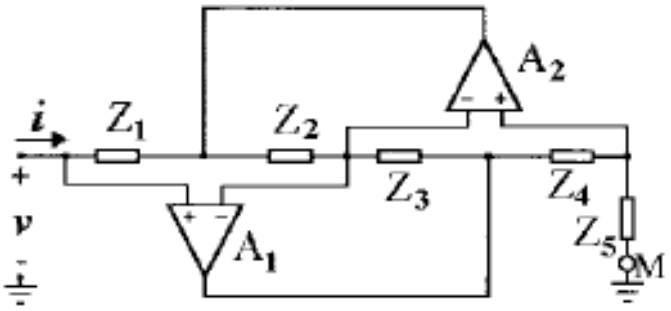

Figure 3. Antoniou's general impedance converter schematic (Leuciue and Goras, 1998).

specifically designed for AC PLC transceivers. However the principles can be applied to DC PLC transceivers.

i) One popular method of improving power transferring is to utilize an equalizer such as proposed in Araneo et al. (2009). This technique boosts the power gain of high frequency and low impedance signals, improving power transferring for broadband PLC modems. However there is a trade off with increased power consumption and it is only ideal for broadband systems.
ii) The second method is to utilize capacitor banks (Choi and Park, 2007) or tapped transformers and inductors (Li et al., 2004) which operate on the principle of electronically tuning the inductor or transformer values to match the transceiver output impedance to the power line channel impedance. The benefit of this design is that a true impedance match is established resulting in no reflections, improved power transferred to the channel and lower supply power consumption. However the downfall of this design is the large amount of board space and limited tuning range.
iii) The last method improving on the tapped trans former and inductors is to replace the tapped inductor with an active inductor (Sun and Amaratunga, 2011; Leuciue and Goras, 1998), as shown in Figure 2.

This circuit eliminates the need for a tapped inductor by replacing it with an active inductor based on Antoniou's general impedance converter shown in Figure 3. By using the active inductors, the impedance tuning range is improved, as well as a smaller PCB and reduced component count being achieved. While there are many benefits to this design, the downside is that a transformer is still required to aid in current carrying ability (Sun and Amaratunga, 2011). This prevents the matching network from being embedded in the modem IC. In the case of PLC in vehicles it can be expensive.

PROPOSED IMPEDANCE MATCHING SOLUTION

Previously in this study, several impedance matching schemes were introduced and their advantages and disadvantages were examined. It emphasized the benefits of active inductors over tapped transformer or tapped inductor solutions for PLC impedance matching. However the need for a transformer makes the active inductor matching network an expensive solution for automotive PLC systems. Therefore a transformerless impedance matching circuit combined with capacitor banks and active inductor topologies was proposed. The tuning range of the proposed matching networks can be improved while allowing for ease of integration in a modem IC.

Figure 4 is the schematic of the proposed impedance matching network. This network construction allows for several different L-matching network configurations. The variable capacitors will be based on a small four capacitor network and the variable inductor will be based on Antoniou's general impedance converter (Antoniou, 1967).

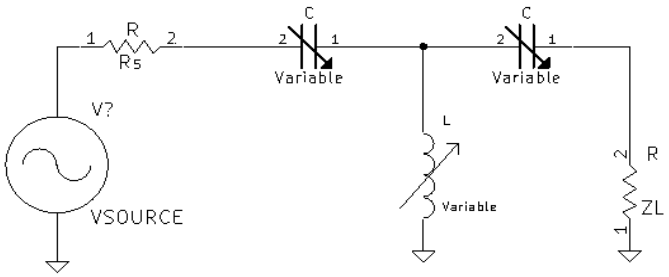

Figure 4. Schematic of the proposed impedance matching network.

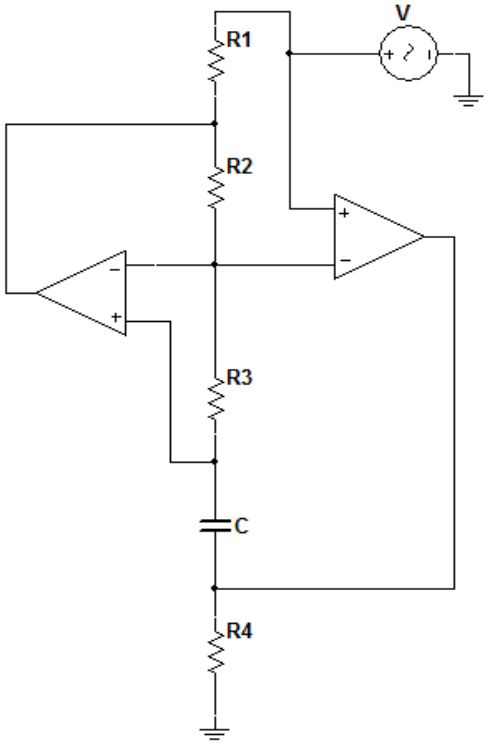

Figure 5. Active inductor schematic.

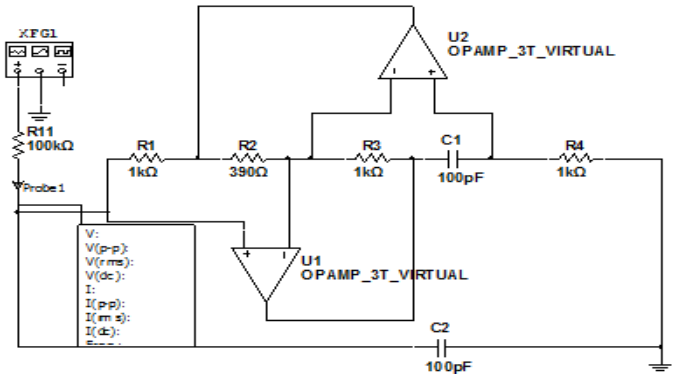

Figure 6. Test bench for the active inductor circuit.

Active inductor

Like the impedance matching network designed in Sun and Amaratunga (2011), the proposed design uses Antoniou's general impedance converter (Antoniou, 1967). Figure 5 shows the modified Antoniou's general impedance converter. The circuit replaces Z_4 with a capacitor and Z_2 and Z_3 with digital potentiometers and the remaining impedances with resistors. The formula for determining the inductance value of the active inductor is as follows:

$$L = \frac{CR_1R_3R_4}{R_2} \quad (1)$$

The tuning range of the active inductor will be limited to the digital potentiometer's resistance range. The selected digital potentiometer is Microchip MCP42100 which has a maximum resistance of 100 $k\Omega$ and 256 taps which means the minimum resistance value is 390 Ω. With R_1, R_3 and R_4 set to 1 $k\Omega$ and C set to 100 pF and R_2 as the digital potentiometer, the tuning range was calculated to be 1.13 to 253 μH.

Active inductor circuit operation

The active inductor was simulated using Multisim 11. Here the active inductor was connected as a parallel RLC tank bandpass filter with a known filtering capacitance as seen in Figure 6. By changing the resistance of R_2 within the bounds of the MCP42100 digital potentiometer the inductance values is given as,

$$\omega = \sqrt{1/C} \quad (2)$$

Substituting $\omega = 2\pi F$ and rearranging (2) for L provides the inductance value for the given R_2 as,

$$L = \frac{1}{4\pi^2F^2C} \quad (3)$$

By changing the value of R_2, the centre frequency of the band pass filter changes as shown in Figures 7 and 8. An important note is that the quality factor of the active inductor as well as the bias point can be adjusted with R_1.

Noise analysis

The effects of the proposed matching network on the noise performance of the PLC networks will be examined here. The noise model shown in Figure 9 is derived from the circuit shown in Figure 5.

The Op amp chosen was the opa2677 by Texas Instruments. This amplifier provides a high output

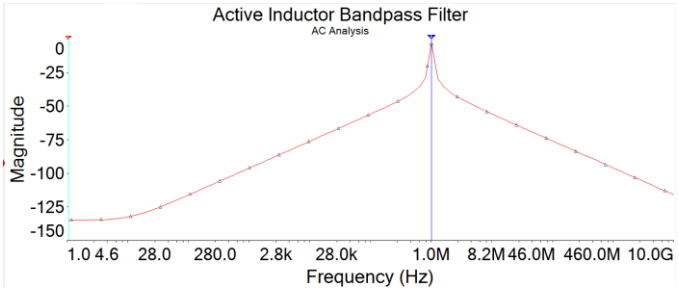

Figure 7. Bandpass filter frequency response with active inductor and $R_2 = 390\ \Omega$.

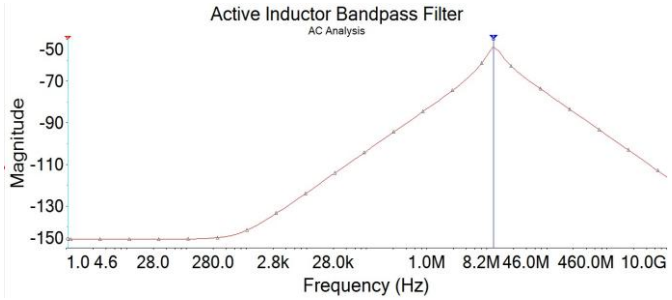

Figure 8. Bandpass filter frequency response with active inductor, $R_2 = 100\ k\Omega$.

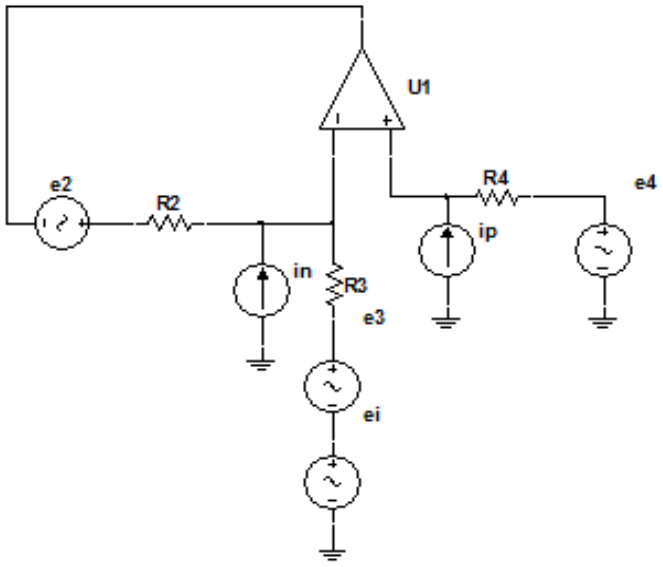

Figure 9. Simplified noise circuit of the proposed impedance matching network.

current of 500 mA, low output impedance, low noise and very large gain bandwidth product of 2 GHz. Unlike traditional voltage feedback op amps, current feedback op amps have a slightly different noise model. It should be noted that resistors R_2 and R_3 are digital potentiometers mcp41100 and mcp41050 by microchip and therefore have slightly different noise characteristics compared to regular model. The key parameters such as input noise, input current noise of the op amp were taken from the datasheet and the shot noise equations were derived from the equivalent circuit as

$$i_n = 24\frac{pA}{\sqrt{Hz}} \qquad i_p = 16\frac{pA}{\sqrt{Hz}} \qquad e_i = 2\frac{nV}{\sqrt{Hz}}$$

where e_i is input noise voltage, i_n is inverting current noise and i_p is non inverting current noise. The input referred spot noise E_i can be expressed as

$$E_i = \sqrt{e_i^2 + \left(i_p R_4\right)^2 + 4KTR_4 + \frac{4KTR_2}{N_G} + \left(\frac{i_n R_2}{N_G}\right)^2} \qquad (4)$$

where N_G is noise gain given by $N_G = 1 + \frac{R_2}{R_3}$ and $4KT = 1.6 \times 10^{-20}\ J$. Then the output noise voltage E_0 is

$$E_o = \sqrt{e_i^2 + \left(i_p R_4\right)^2 + 4KTR_4 + 4KTR_2N_G + (i_n R_2)^2}$$

From the equations above, it was calculated that the opa2677 output shot noise is $E_o = 2.43\frac{\mu V}{\sqrt{Hz}}$ and the input noise is $E_i = 29.48\frac{nV}{\sqrt{Hz}}$ which translates to E_0 =5.7 mV and E_i=6.91 μV at a frequency of 5.5 MHz. The noise values calculated on the input are insignificant due to the modems threshold of 20 mV_{pp} sensitivity. However, the output noise generated by the system is quite extensive with strength of 5.7 mV_{rms} or 16.12 mV_{pp}. This comes into the range of the SIG60s sensitivity level. Therefore this impedance matching network would be too noisy to be used on the receiving end. However on the transmitter side the signal driven onto the line is very large up to 3 V_{pp} which is larger than the noise generated by the matching circuit. Therefore the benefits of the improvement of power transferring are still valid on the transmitting end but not so much on the receiving end.

With the active inductors operation and noise characteristics determined, the proposed impedance matching network can be tested. Next is a presentation of simulation results of the proposed impedance matching network.

SIMULATION RESULTS

Multisim 11 is used for the simulation. The results will be

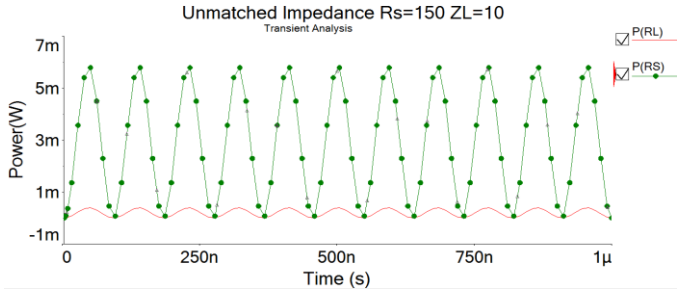

Figure 10. Input output power waveform for 150 Ω source impedance and 10 Ω load impedance before matching.

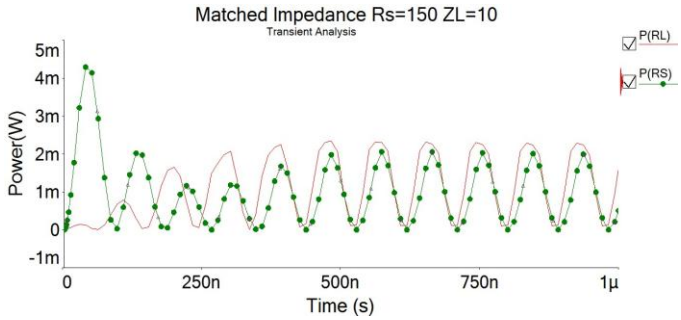

Figure 11. Input output power waveform for 150 Ω source impedance and 10 Ω load impedance after matching.

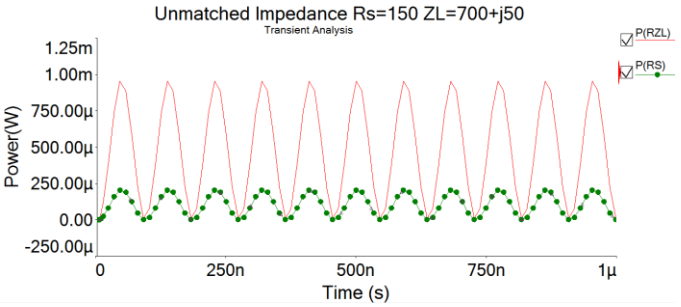

Figure 12. Input output power waveform for 150 Ω source impedance and 700 Ω + j50 Ω load impedance before matching.

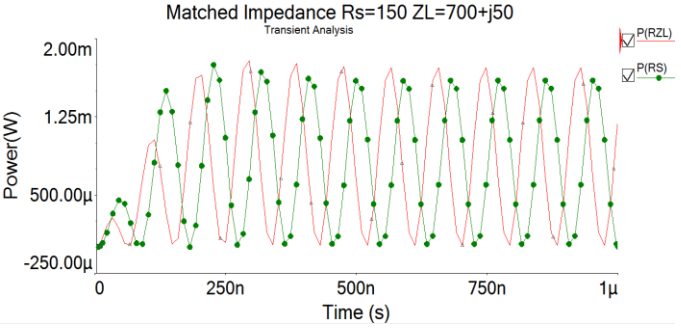

Figure 13. Input output power waveform for 150 Ω source impedance and 700 Ω + j50 Ω load impedance after matching.

obtained by observing the output power waveforms to determine if a match is established. The carrier frequency used for the simulations will be 5.5 MHz and the output impedance of the signal source will be 150 Ω. The simulations consist of four scenarios as:

1) real to real match with load impedance lower than the source impedance;
2) real to inductive impedance match;
3) automotive load impedances; and
4) variable load impedances.

These simulations will help to determine the matching networks viability for operation in automotive applications.

Real Source Impedance Real Load Impedance

The first test is to match a 150 Ω source impedance to a 10 Ω load impedance. This impedance value represents an ideal case, as most impedances found on the power line will have a reactive component. However the circuits line drive capability and tuning range need to be examined to determine the matching networks viability. Figure 10 shows the power waveforms of R_S and Z_L before impedance matching. As expected most of the power is dissipated in the source resistor R_S and very little is transferred to Z_L. Figure 11 is the result after applying the proposed impedance matching network. As expected, both input and output waveforms are closely related in power, meaning a successful match was established.

Real Source Impedance Complex Load Impedance

The second test was to match a 150 Ω source impedance to a complex load impedance of 700 Ω + j50 Ω. This scenario represents a realistic matching condition found on a PLC network, as the complex component of the channel impedance is usually inductive. Figure 12 shows the power waveforms of R_S and Z_L before impedance matching. As before, most of the power is dissipated in Z_L. Figure 13 shows the power waveforms after applying the matching network. As expected, both R_S and Z_L share the power equally, meaning a successful match is established.

Automotive Load Impedances

The third test is to examine the matching networks ability to operate with the impedances of automotive devices. The tests are to match the 150 Ω signal generator impedance to the impedances of a car battery and various lights of the vehicle. As the PLC modem may be connected close to t hese devices, the low

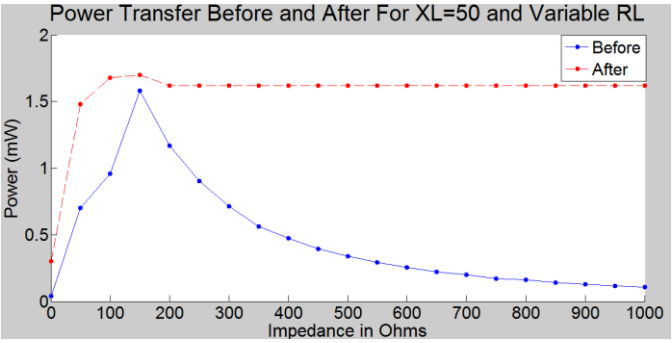

Figure 14. Power delivered to load before and after impedance matching network with variable real component and 50 Ω reactive component.

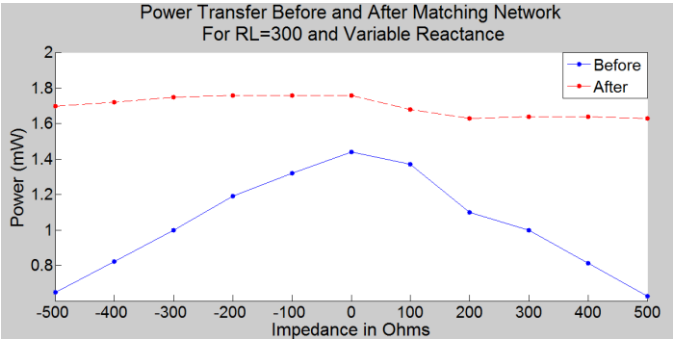

Figure 15. Power delivered to load before and after impedance matching network with 300 Ω real component and variable reactive component.

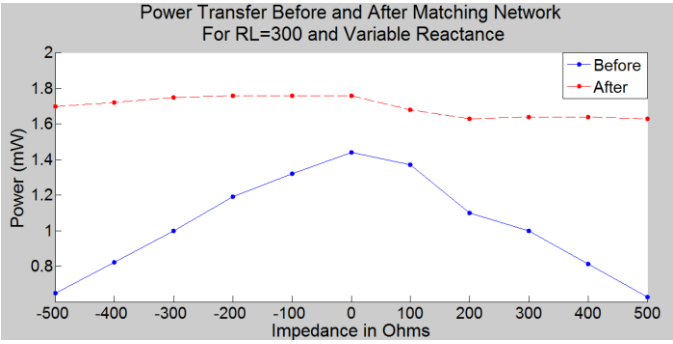

Figure 16. Power delivered to load before and after impedance matching network with 20 Ω real component and variable reactive component.

impedances of these devices could adversely affect the operation of the matching network.

In these tests the output power was observed before applying the matching network and after applying the matching network. From the observed power levels, the improvement factor is calculated as the ratio of the power transferred after matching to the power transferred before matching. The impedance values of the components are determined through the measurements in Taherinejad et al. (2011) for a frequency of 5.5 MHz. Table 1 shows the results of the matching network when matched to various automotive devices.

The results from Table 1 show the impedance matching network improves the power transferred of the PLC modem to the channel with multiple folds. A point to note would be that the improvement drops off as the impedance increases closer to the value of the source impedance. This is explained by noting that the real part of the impedance is closer in value to the source impedance, meaning the device is better matched compared to the devices with smaller impedances.

Variable Load Impedances

The fourth test was to examine the matching networks ability to perform impedance matches over a range of impedances found on automotive power lines as the impedances observed on the automotive power line can vary from close to 0 Ω to 1 kΩ, with varying reactive components (Mohammadi et al., 2009; Reuter et al., 2011). Therefore the tuning range of the matching network must be examined to determine if this design is viable option for automotive PLC impedance matching.

In these tests the proposed matching network will attempt to match a 150 Ω signal generator impedance to 1) variable real impedance and j50 Ω reactive component; 2) 300 Ω real impedance and variable reactive impedance; and 3) 20 Ω and variable reactive impedance. Figures 13, 14 and 15 will show the power delivered to the load before and after the matching network is applied.

The results from Figures 13, 14 and 15 shows that the matching network improves the power transfer of the signal generator to the load over the expected range of automotive impedances. The results show the proposed matching network has the ability to provide matches over most expected impedance on automotive power lines. A point to note is that the matching network will have trouble matching large capacitive loads <-j100 Ω with small real values. This is due to the need for extremely large value capacitors in the capacitor banks which would make the size of the proposed design impractical. However since most impedance found in automotive power lines have inductive components (Taherinejad et al., 2011), this means the need to match large capacitive impedances will be very rare.

Conclusions

An adaptive impedance matching network for automotive PLC was proposed based on Antoniou's general impedance converter in this paper. It was shown that the

Table 1. Automotive impedance matching results.

Device	State	Impedance (Ω)	Power transfer before (μW)	Power transfer after	Improvement factor
Car Battery	N/A	1 + j6	42.93	302 μW	7.0
Headlights	Off	0.32 + j5.97	16.17	122.6 μW	7.6
Headlights	On	2.74 + j5.97	122.7	734 μW	5.98
Rear lights	Off	6.59 + j9.3	260	1.27 mW	4.88
Rear lights	On	25.2 + j9.3	805	1.68 mW	2.08

proposed matching network has the ability to provide successful impedance matches with a number of automotive loads and channel impedances. However for devices such as the rear lights, which had impedances closer to the source impedance the benefits of the matching network were reduced. It was discovered that the proposed network may not be an attractive solution for automotive PLC applications due to the expensive components, large PCB area and noise characteristics. However the proposed design does show promise if it is integrated into the PLC modems IC, by doing this the issues mentioned above are eliminated. It can be seen that there are benefits to having impedance matching for PLC networks; however more research needs to be done to make it a cost viable solution.

ACKNOWLEDGEMENT

The authors sincerely acknowledge the support from Ontario Centre of Excellence (OCE) under Grant numbers 11076 and 11759.

Conflict of Interest

The authors have not declared any conflict of interest.

REFERENCES

Benzi F, Facchinetti T, Nolte T, Almeida L (2008). To- wards the Powerline Alternative in Automotive Applications. IEEE International Workshop on Factory Communication Systems. PMCid:PMC3166804

Sun Y, Amaratunga GAJ (2011). High-Current Adaptive Impedance Matching in Narrowband Power-line Communication Systems. IEEE International Sympo sium on Power Line Communications and Its Appli- cations (ISPLC).

Maniati EV, Skipitaris D (2007). Robust Detection in Power Line Communication for OFDM and non- Rayleigh Fading Channels. IEEE International Sym- posium on Power Line Communications and Its Applications.

Fallows K, Yazdani J, Brown B, Honary B(1998).Data Protection and Transmission Over Low Voltage in- House Power Line Channel. International Sympo- sium on Power-line Communications and its Applications.

Araneo R, Celozzi S, Lovat G (2009). Design of Impedance Matching Couplers for Power Line Communication. IEEE Internation Symposium on Electromagnetic Compatibility.

Choi WH, Park CY (2007). A Simple Line Coupler with Adaptive Impedance Matching for Power Line Communication. IEEE International Symposium on Power Line Communications and Its Applications.

Choi WH, Park CY, Jung KW (2008). Coupling Ciruitary for Impedance Adaptation in Power Line Communications using VCGIC. IEEE International Symposium on Power Line Communications and Its Applications.

Li Q, She J, Feng Z (2004). Adaptive Impedance Matching In Power Line Communication. ICMMT 4th International Conference on Microwave and Millimeter Wave Technology.

Mohammadi M, Lampe L, Lok M, Mirabbasi S, Mir- vakili M, Rosales R, Van Veen P (2009). Measure- ments Study and Transmission for In-vehicle Power Line Communication. IEEE International Symposium on Power Line Communications and Its Applications. http://dx.doi.org/10.1109/ISPLC.2009.4913407

Taherinejad N, Rosales R, Mirabbasi S, Lampe L (2011). A study on access impedance for vehicular power line communications. IEEE International Symposium on Power Line Communications and Its Applications. Pp. 440-445.

Leuciue A, Goras L (1998). New general immitance converter JFET voltage-controlled impedances and their applications to controlled biquads synthesis. IEEE Transactions on Circuits and Systems I: Fundamental Theory. Appl. 45(6):678-682.

Antoniou A (1967). Gyrator using operational amplifier. Electr. Lett. 3(8):350-352. http://dx.doi.org/10.1049/el:19670270

Taherinejad N, Rosales R, Mirabbasi S, Lampe L (2012). On the Design of Impedance Matching Circuits for Vehicular Power Line Communication Systems. IEEE International Symposium on Power Line Communications and Its Applications. pp. 322-327.

Despande S, Prasanna IV, Panda SK (2013). An Adaptive Impedance Matching Technique for Narrowband Power Line Communication in Residential Smart Grids. Int. J. Eng. Res. Technol. (IJERT). 2(9):157-161.

Sibanda MP, Janse van Rensburg PA, Ferreira HC (2011). Impedance Matching with Low-Cost, Passive Components for Narrowband PLC. International Symposium on Power Line Communications and Its Applications. pp. 335-340.

Reuter M, Tenbohlen S, Ko¨ hler, Ludwig A (2011). Impedance Analysis of Automotive High Voltage Net- works for EMC Measurements. 10th International Symposium on Electromagnetic Compatibility. pp. 106-111.

Journal of Electrical and Electronics Engineering Research

Related Journals Published by Academic Journals

- *Journal of Engineering and Technology Research*
- *International Journal of Water Resources and Environmental Engineering*
- *Journal of Civil Engineering and Construction Technology*
- *International Journal of Computer Engineering Research*
- *Journal of Chemical Engineering and Material Science*
- *Journal of Engineering and Computer Innovations*
- *Journal of Mechanical Engineering Research*
- *Journal of Petroleum and Gas Engineering*

academicJournals